



Scholars Research Library

Der Pharma Chemica, 2013, 5(3):141-155  
(<http://derpharmachemica.com/archive.html>)



ISSN 0975-413X  
CODEN (USA): PCHHAX

## Adsorption studies of lead (II) and nickel (II) ions on chitosan-G-polyacrylonitrile

Shanmugapriya A<sup>a</sup>, Hemalatha M<sup>a</sup>, Scholastica B<sup>a</sup> and Augustine Arul Prasad T<sup>b</sup>

<sup>a</sup>Department of Chemistry, Auxilium College For Women, Vellore, Tamilnadu, India

<sup>b</sup>Post Graduate and Research Department of Chemistry, D. G. Vaishnav College, Arumbakkam, Chennai

### ABSTRACT

In the present work, graft copolymerization of polyacrylonitrile onto chitosan has been carried out in the presence of ceric ammonium nitrate redox initiator. Chitosan has been used as an adsorbent for the removal of heavy metal ions from aqueous solution through adsorption process. The property of chitosan is enhanced by grafting. The prepared copolymer was characterized by FTIR, XRD, TGA and SEM. The effect of pH, contact time and amount of adsorbent dose were also investigated. The experimental data were fitted to Freundlich and Langmuir adsorption isotherms.

**Key words:** Grafting, Chitosan-g-polyacrylonitrile, Adsorption isotherm.

### INTRODUCTION

Water is an essential matter to human and other living organisms. Water is polluted in many ways like effluents from leather and chemical industries, electroplating industries and dye industries[1]. Effluents from textile, leather, tannery, electroplating, galvanizing, pigment and dyes, metallurgical and paint industries and other metal processing and refining operations at small and large-scale sector contains considerable amount of toxic metal ions. These toxic metals ions are not only potential human health hazards but also to other life forms[2]. Although individual metals exhibit specific signs of their toxicity, the following have been reported as general signs associated with cadmium, lead, arsenic, mercury, zinc, nickel, copper and aluminium poisoning: gastrointestinal (GI) disorders, diarrhoea, stomatitis, tremor, haemoglobinuria causing a rust-red colour to stool, ataxia, paralysis, vomiting and convulsion, depression, and pneumonia when volatile vapours and fumes are inhaled[3]. Several methods have been used to purify the water like sedimentation, filtration, ultra filtration, precipitation, ion exchange, electro coagulation, electro dialysis, and reverse osmosis in cleaning wastewater[4]. Hence, the disadvantages associated with traditional methods of heavy metal removal like incomplete metal removal, high energy requirement, generation of toxic sludge and other waste products have made it important to look of other cost-effective treatment methods[5]. Moreover, traditional methods of heavy metal removal are not so efficient when metals are present in concentrations less than 100mg/L. Hence, attention is being focused to the development of alternative methods of heavy metal removal like bioremediation. One of such processes is adsorption [6, 7].

Recently numerous approaches have been studied for the development of cheaper and more effective adsorbents containing natural polymers. The removal of metals, compounds and particulates from solution by biological material is recognized as an extension to adsorption and is named as biosorption[8]. Various mechanisms active in biosorption are chemisorption, physical adsorption, micro precipitation and oxidation/reduction. Biosorbents can be obtained from various sources like – seaweeds, microorganisms, activated sludge, fermentation wastes etc [9, 10].

Many biosorption such as fungi[11], Algae, Seaweeds[12], Microorganisms[13] and several biopolymers [14] have been utilized in the removal of heavy metals from wastewater. The polysaccharides are renewable resources which are currently being explored intensively for their applications in water treatment [15]. Among the polysaccharide compounds such as chitin starch and their derivatives chitosan[16] deserve particular attention. These polysaccharides are abundant, renewable, and biodegradable, low-cost and are the best choice in water treatment and useful tool for protecting the environment [17].

Chitin because of its insolubility is rarely subjected to chemical reactions except for the preparation of chitosan by deacetylation. Khor[18] has stated that 21 st century can be the century of chitin taking a place as an extra ordinary material because chitin and its derivatives have exhibited high potential in a wide variety of fields (Medical, pharmaceutical, cosmetics, food industry, agriculture, environmental protection)[19]. Chitosan can be dissolved in only acidic solutions through the interaction between  $H^+$  and  $NH_2$ , but it is insoluble under higher pH conditions. It is also of limited solubility in organic solvents. In order to sort the above problems, chemical modification affords a wide range of novel chitosan derivatives. Among the various methods of modification graft copolymerization is an attractive technique to modify the chemical and physical properties of chitosan[20].

Grafting of chitosan allows the formation of functional derivatives by covalent binding of a molecule, the graft, on to the chitosan backbone. Chitosan has two types of reactive groups such as free amino groups and hydroxyl groups that can be grafted [21].

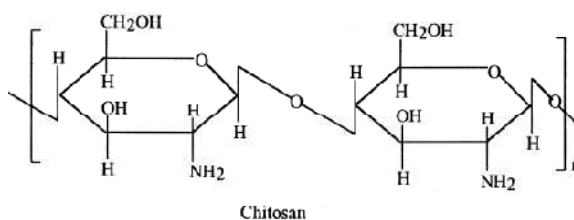


Figure 1

Chitosan grafted with polyacrylonitrile has been further modified to yield amidoximated chitosan, a derivative having a higher adsorption capacity for copper, lead, nickel compared to cross linked chitosan. Adsorption of Cu (II) and Ni (II) from metal solution using cross linked chitosan-g-polyacrylonitrile copolymer was conducted and the results showed that it is a favorable adsorbent for the removal of heavy metal ions[22].

Adsorption of Cu (II) and Cr (VI) from metal solutions using UV assisted oxidative process chitosan-g-polyacrylonitrile copolymer was conducted and the results showed that it is a favorable adsorbent for the removal of heavy metal ions[23].

In the present study, we have synthesized graft copolymer chitosan -g-polyacrylonitrile using ceric ammonium nitrate as the initiator. The prepared graft copolymer was subjected to various analytical techniques such as FTIR, XRD, TGA, and DSC to confirm the grafting. Also we investigated the polymerization variables such as initiator concentration, monomer concentration and reaction temperature. This graft copolymer will be highly useful for various application fields including wastewater treatment. In present work efficacy of chitosan - g - polyacrylonitrile for treating heavy metals solution was attempted and found successful.

## MATERIALS AND METHODS

Chitosan was obtained from India Sea Foods, Cochin, Kerala, India, Acrylonitrile, Ceric ammonium nitrate (CAN) and all other chemicals used in the experiment were of analytical grade. Chitosan-g-polyacrylonitrile was prepared using CAN as initiator, Acrylonitrile as a monomer, chitosan as a polymer. A 2% w/v solution of chitosan was prepared in 2% aqueous acetic acid. A solution of 0.1M CAN in 10 ml of 1 N nitric acid was added followed by a known amount of acrylonitrile drop by drop with continuous stirring. After a specified time, the product was precipitated by pouring into (2N) sodium hydroxide solution with vigorous stirring. The precipitate was washed with distilled water several times and filtered.

In the present study chitosan has been graft copolymerized with acrylonitrile with an aim to develop a product, which could be used for wastewater treatment at different temperatures such as 30°C, 50°C, 70°C, & 90°C. The samples were subjected to spectral studies.

#### FOURIER TRANSFORM INFRARED SPECTROSCOPY (FTIR)

In the present investigation, transmittance spectra was used to quantify the characteristic peak of the synthesized grafting copolymer in the range between 4000-400  $\text{cm}^{-1}$  using Thermo Nicolet AVATAR 330 Spectrophotometer, using KBr pellet method. The FTIR spectra were normalized and major vibration bands were identified associated with the main chemical groups.

#### THERMOGRAVIMETRIC ANALYSIS (TGA)

Thermo gravimetric analysis was conducted to measure the weight loss of the copolymers on a DTG-60 instrument at a heating rate of 10°C per minute for in nitrogen atmosphere. The weight loss at different stages was analyzed.

#### X-RAY DIFFRACTION TECHNIQUE (XRD)

Room temperature low angle X-ray diffraction (XRD) patterns of the chitosan-g-polyacrylonitrile copolymers were studied using X-ray powder diffractometer (XRD –MINI FLEX II) using a Ni – filtered Cu  $K\alpha$  X-ray radiation source. The relative intensities were recorded within the range of 10° – 90° (2 $\theta$ ) at a scanning rate of 5°  $\text{min}^{-1}$ .

#### SCANNING ELECTRON MICROSCOPY (SEM)

The surface morphology of the copolymers was observed with scanning electron microscopy to verify the compatibility of the chitosan copolymer. For the analysis, the samples were cut into pieces of various sizes and wiped with a thin gold – palladium layer by a sputter coater unit and the cross section topography was analyzed with a Cambridge stereo scan 440 scanning electron microscope (SEM, Leica, and Cambridge, UK).

### RESULTS AND DISCUSSION

As reported in the literature[24], the monomer conversion was found to be between 70 and 80 % after 2h of reaction at 70°C. The grafting efficiency of chitosan was increased in the present work where 80% of yield has been obtained in one hour. Various Cs-g-PAN samples were prepared by changing the reaction temperatures at 30°C, 50°C, 70°C, & 90°C characterized completely using FTIR, XRD, TGA and SEM.

The samples were prepared by changing the various temperatures at 30°C, 50°C, 70°C, and 90°C. Out of the four samples, the sample prepared at 50°C showed high grafting yield. Hence 50°C was found to be optimum temperature for grafting; the samples were characterized by FTIR, TGA, XRD, and SEM. The yield of copolymer is given in table 1 and figure 2. The results are discussed below.

Table 1 Determination of grafting efficiency with temperature

<i>Wt of chitosan-0.5gms, Wt of AN-0.5gms,</i>				
S.No	Temperature (°C)	Amount of copolymer (g)	% Grafting Efficiency	Grafting yield %
1	30	0.6213	55.40	24.26
2	50	0.7104	58.69	42.08
3	70	0.6673	57.16	33.46
4	90	0.6150	55.15	23.00

#### The FTIR spectra of chitosan and Chitosan-g-polyacrylonitrile

The FT-IR Spectra of chitosan showed a absorption band at 3426.19 $\text{cm}^{-1}$  due to the presence of N-H stretching, O-H stretching, polymeric association and intermolecular hydrogen bonding and C=O vibration at 1646.53 $\text{cm}^{-1}$  where as Chitosan-g-PAN copolymer of 30°C, 50°C, 70°C, & 90°C. shows the prominent peaks at 3429.02 $\text{cm}^{-1}$ , 3456.44 $\text{cm}^{-1}$ , 3454.51 $\text{cm}^{-1}$ , and 3442.94 $\text{cm}^{-1}$ , 1567.16 $\text{cm}^{-1}$ , 1535.34 $\text{cm}^{-1}$ , 1543.05 $\text{cm}^{-1}$ , and 1537.27 $\text{cm}^{-1}$ , and 1412.43 $\text{cm}^{-1}$ , 1386.82 $\text{cm}^{-1}$ , 1373.32 $\text{cm}^{-1}$ , and 1375.25 $\text{cm}^{-1}$ , 1078 $\text{cm}^{-1}$ , 1080.14 $\text{cm}^{-1}$ , and 1078.21 $\text{cm}^{-1}$ . The broad band at 3456.44 $\text{cm}^{-1}$ , 3454.51 $\text{cm}^{-1}$ , and 3442.94 $\text{cm}^{-1}$ , shows the presence of NH stretching, OH stretching, polymeric association and inter molecular hydrogen bonding. There was a shift towards lower wave length region during copolymer formation (3454.51 $\text{cm}^{-1}$ ). The peaks at 1386.82 $\text{cm}^{-1}$  and 1373.32 $\text{cm}^{-1}$  was due to  $-\text{CH}_2$  vibration attributed to pyranose ring in chitosan. The disappearance of the peak in the copolymer showed that the grafting of polymers had taken place.

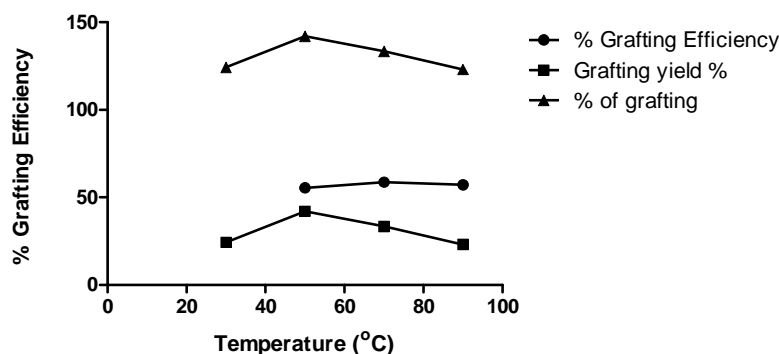


Fig 2 Determination of grafting efficiency with temperature

Chitosan-g-PAN showed the peaks at 1078.21 and 1080.14  $\text{cm}^{-1}$  shows the presence of C-O-C linkage, respectively. The successful polymeric linkage in the copolymer is confirmed by the amide bands at 1535.34 and 1543.05  $\text{cm}^{-1}$  as well as glycosidic bands (C-O-C) of chitosan.

The grafting yield at 50°C was very high and is optimum for grafting and is confirmed by the intensity of the peak obtained at 1535.34  $\text{cm}^{-1}$  is high due to N-H bending. Hence from the results it is confirmed that the grafting has taken place between chitosan and from the spectra it is evident that acrylonitrile got attached to the chitosan moiety at the amino group.

#### The proposed Structure for chitosan-grafted-PAN

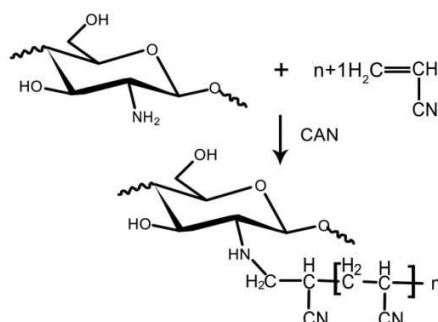


Figure 3

#### TGA Thermal Analysis of Cs-g-PAN Copolymers

TGA thermogram details of chitosan with 92% degree of deacetylation are shown in **Figure 4**. About 50% of chitosan decomposed at around 700°C. Two weight losses were observed in the chitosan TGA curve. The first weight loss at around 200° -350°C was due to the detachment of the entangled chitosan chains. The second degradation around 450-700 may be due to the degradation of chitosan molecule. At the end of the experiment nearly 30% of the sample remained as residue showing the higher thermal stability of chitosan.

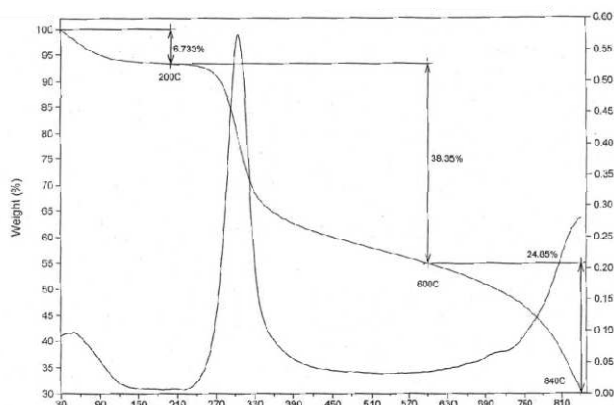


Fig 4 TGA for Chitosan

## TGA of Chitosan-g- PAN copolymer at 30°C

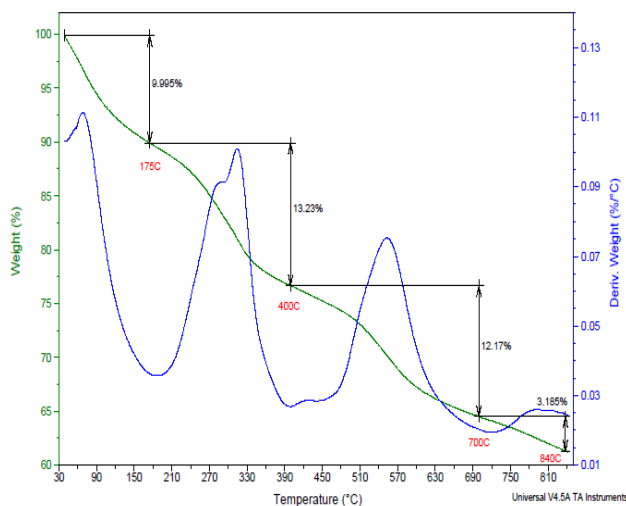


Fig 5 TGA of Chitosan-g- PAN copolymer at 30°C

**Figure 5** shows the TGA thermogram details of Chitosan-g-PAN copolymer by varying temperature at 30°C. 9% weight loss occurred at 176°C was due to the loss of water from the sample (Huicai et al., 2006). Around 30% of the sample disintegrated in the temperature range of 640°C. Maximum weight loss occurred at the temperature range 90°C-400°C. At the end of the experiment at 840°C, 61.42% of the copolymer remained as residue. **Figure 6** represent the thermogram details of Chitosan-g- PAN copolymer by varying temperature at 50°C. The 5% weight loss in the copolymer at 100°C was due to loss of water in the sample. Around 71.51% of the sample gets disintegrated in the temperature range of 281.36°C. At the end of the experiment at 800°C, 28.49% of the copolymer remained as residue showing the high thermal stability of the copolymer when compared to sample containing 70°C and 90°C.

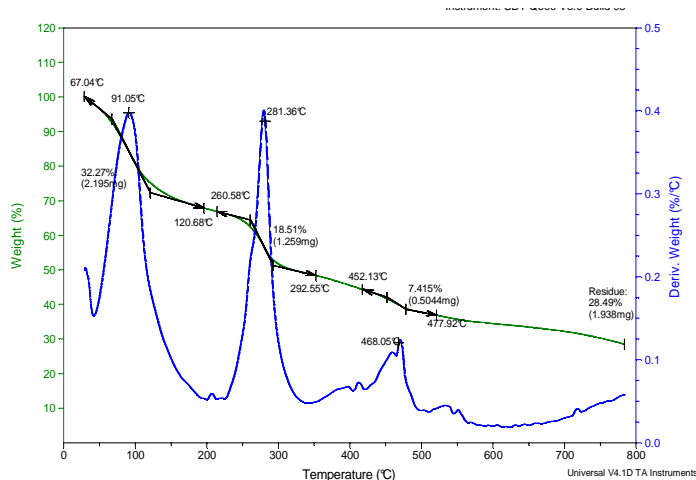


Fig 6 TGA of Chitosan-g- PAN copolymer at 50°C

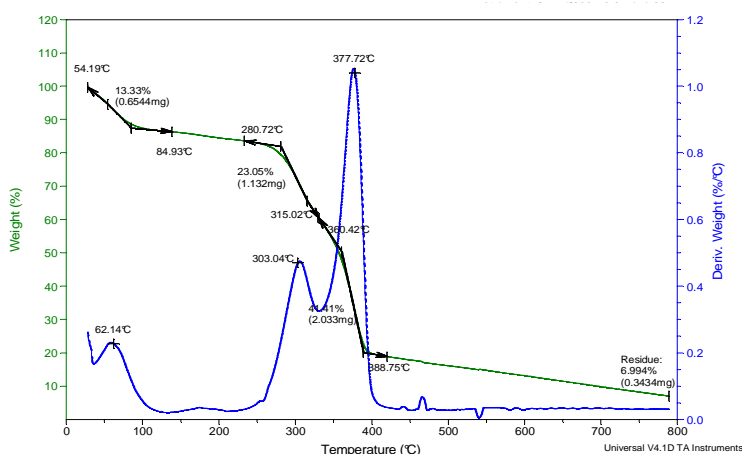


Fig 7 TGA of Chitosan-g- PAN copolymer at 70°C

Figure 7 show the thermogram details of Chitosan-g-PAN copolymer by varying temperature at 70°C. At the temperature of 800°C around 93.006% of the sample had disintegrated. At the end of the experiment 6.994% of the copolymer remained as a residue. The maximum weight loss occurred in the temperature range of 280°C-400°C. Around 80% of the sample got disintegrated in the temperature range of 400°C. From there, only a shallow weight loss takes place with increase in temperature. The sample is less stable compared to sample having 70°C.

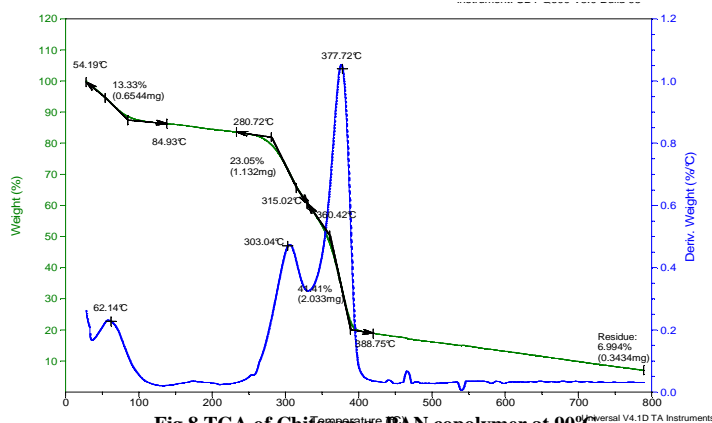


Fig 8 TGA of Chitosan-g- PAN copolymer at 90°C

Figure 8 show the thermogram details of the Chitosan-g-PAN copolymer by varying reaction temperature at 90°C. 13.33% weight loss of the copolymer occurred at 62.14°C was due to the loss of moisture from the sample. Around 93% of the sample gets disintegrated in the temperature range of 377.7°C. Maximum weight loss occurred at the temperature range 315.02°C-388.25°C. At the end of the experiment at 800°C, 6.994% of the copolymer remained as residue.

X- ray diffraction Studies (XRD) for chitosan and Chitosan-g PAN

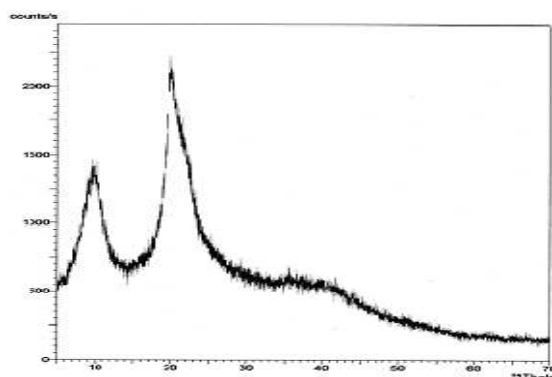


Fig 9 XRD of chitosan

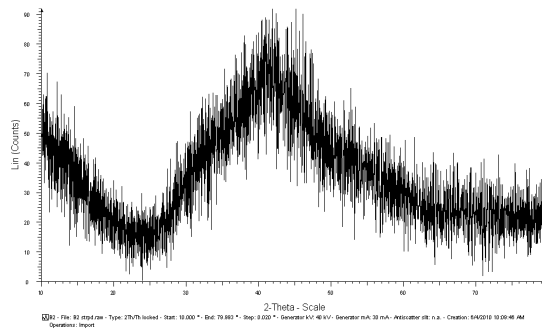


Fig 10 Chitosan-g-PAN copolymer at 30°C

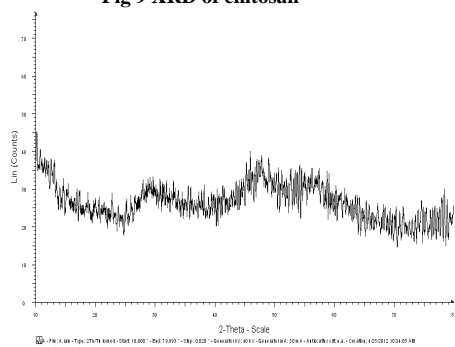


Fig 11 chitosan-g-PAN copolymer at 50°C

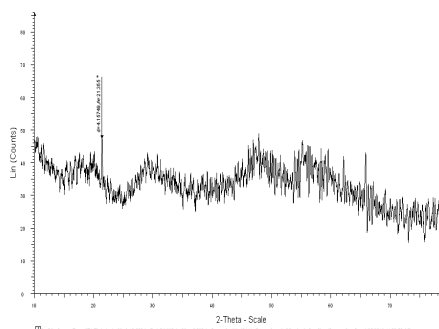


Fig 12 Chitosan-g-PAN copolymer at 70°C

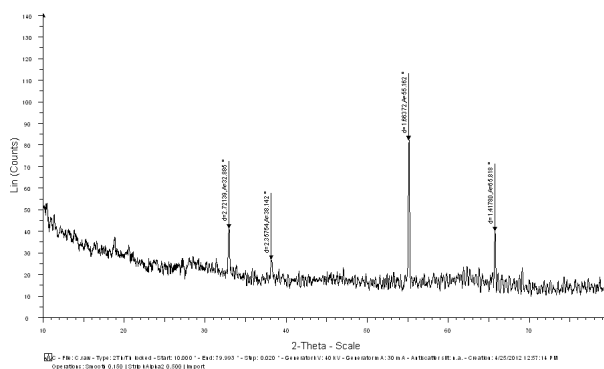


Fig 13 chitosan-g-PAN copolymer at 90°C

Figures 10-13 show the XRD pattern of chitosan-g-PAN copolymer prepared by varying temperature. The XRD pattern of 30°C, 50°C, 70°C, and 90°C show sharp peaks at 2θ=42, 41, 41, 43 respectively. From the nature of

peaks obtained it was concluded that the copolymers 30°C, 50°C, 70°C, and 90°C were found to have semi crystalline nature. The typical crystalline peak of chitosan that appeared at  $2\theta=20^\circ\text{C}$  had been shifted around  $41^\circ\text{C}$  and the peak at  $10^\circ\text{C}$  had disappeared showing the copolymer formation with increase in concentration of PAN in graft copolymer.

### 3.4 Scanning Electron Microscopy (SEM)

The surface morphology of chitosan characterized by SEM (Figure 14 and 15) indicated micro porous structure[25]. Grafting considerably modified chitosan morphology, and also its physical, chemical and biodegradable characteristics, which varied with respect to the nature of the synthetic side chains incorporated.

#### Morphological studies of copolymer:

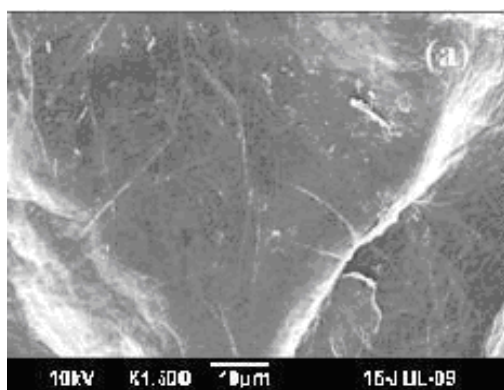


Figure 14 Surface morphology of chitosan

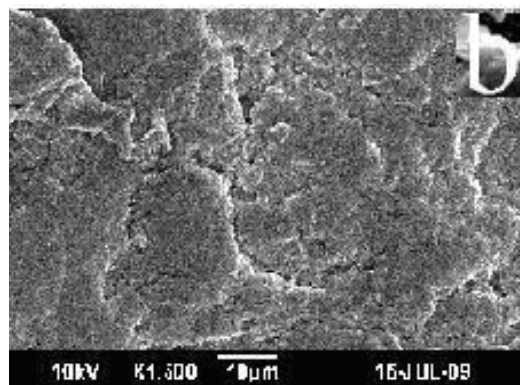


Figure 15 Surface morphology of Chitosan-g-PAN

The SEM image of chitosan shows smooth surface, because there are stronger interaction between the chitosan molecules. The copolymerization of polyacrylonitrile modified the surface morphology of chitosan significantly making it useful for water treatment. The SEM image of copolymer revealed that uniform distribution of polyacrylonitrile might be improving that characteristic nature of chitosan as well as polyacrylonitrile. This characteristic membrane may be responsible to allow water with greater adsorbing property.

#### Adsorption studies using chitosan-g-polyacrylonitrile copolymer for the removal of nickel and lead ions from metal solutions

The presence of heavy metals in environment is of major concern because of their transformation from relatively highly toxic even in lower concentration. Thus it is necessary to control emissions of heavy metals into environment. Chitosan and its derivatives have been extensively investigated as biosorbent for removal of heavy metals.

In this investigation chitosan has been modified by copolymerization with polyacrylonitrile to improve the properties and increase their adsorption efficacy. Hence attempts have been made to investigate the metal adsorbing capacity of chitosan-g-polyacrylonitrile copolymer for heavy metals lead and nickel removal from metal solutions.

#### Batch adsorption studies

The removal of metal ions (lead & nickel) from metal solutions was carried out using chitosan-g- polyacrylonitrile by batch adsorption studies.

#### Effect of adsorbent dose

The study of effect of adsorbent dose on metal adsorption has shown in figure16. That adsorption had increased for both the metals with increase in amount of chitosan-g-polyacrylonitrile. The effect of the amount of adsorbent on the removal of  $\text{Pb}^{2+}$  and  $\text{Ni}^{2+}$  ions shown in figure. It is observed that the removal of metal ions increases with an increase in the amount of adsorbent. The amount of adsorbent dose was varied from 0.5g-5g for lead, minimum percentage removal was 17.3% for a dose of 0.5gm and maximum value of 74.8% for the dose of 5gm, whereas nickel, minimum percentage removal was 18.4% for a dose of 0.5gm and maximum value of 78.7% for the dose of 5gm, as shown in figure. The number of adsorption sites or surface area increases with the weight of adsorbent and

hence results in a higher percent of metal removal at a high dose. Among the two metals nickel gets adsorbed at higher rate than lead.

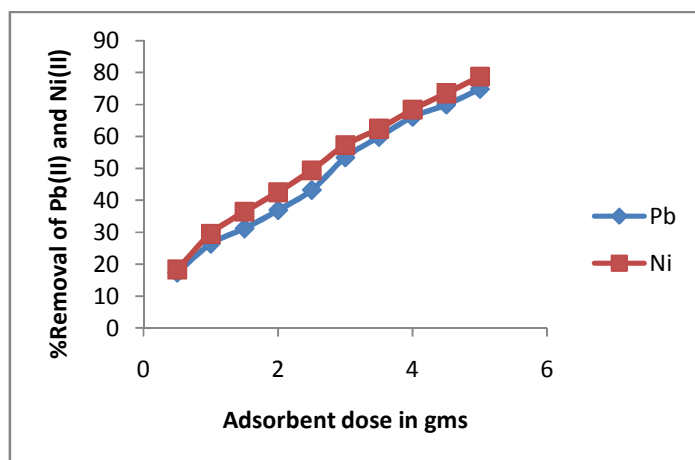


Fig 16 Effect of adsorbent dose on the removal of Pb (II) and Ni(II)

#### Effect of pH

The pH of the solution affects the surface charge of the adsorbents. The pH is one of most important environmental factor influencing not only site dissociation, but also the solution chemistry of the heavy metals. The pH value of the solution is an important controlling parameter in the adsorption process.

It was observed that with the increase in the pH of the solution, the extent of metal ions removal increased for the adsorbent. The extent of removal of Pb (II) and Ni(II) was investigated by varying the pH from 2.0 to 8.0 and the results are shown in table3.6 and figure3.10. It is observed that pH significantly affects the adsorption process of both metals. The best results were obtained at pH4.5 for lead and pH5.5 for nickel. Increase in metal removal with increase in pH can be explained on the basis of a decrease in competition between proton and metal cations for same functional groups and by decrease in positive surface charge, which results in a lower electrostatic repulsion between surface and metal ions. Decrease in adsorption at higher pH is due to formation of soluble hydroxyl complexes.

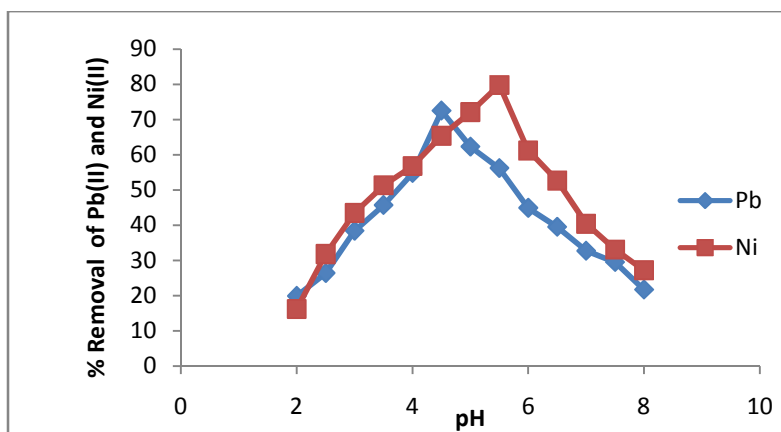


Fig 17 Effect of pH on the removal of Pb(II) and Ni(II)

#### Effect of contact time

The effect of contact time on adsorption was studied and the results as shown in figure3.11. Increase in removal efficiency with increase in time of contact can be attributed to the fact that more time becomes available for metal

ions to make an attractive complex with chitosan-g-polyacrylonitrile. Figure 3.11 depicts that it was found that the removal of metal ions increased with increase in contact time to some extent. This means that a large amount of vacant adsorption sites were available at this stage. Further increase in contact time does not increase the uptake due to unavailability of adsorption sites of the adsorbent materials. At first adsorption capacity was a slow process then increases rapidly, it attains equilibrium and saturation gives constant adsorption value.

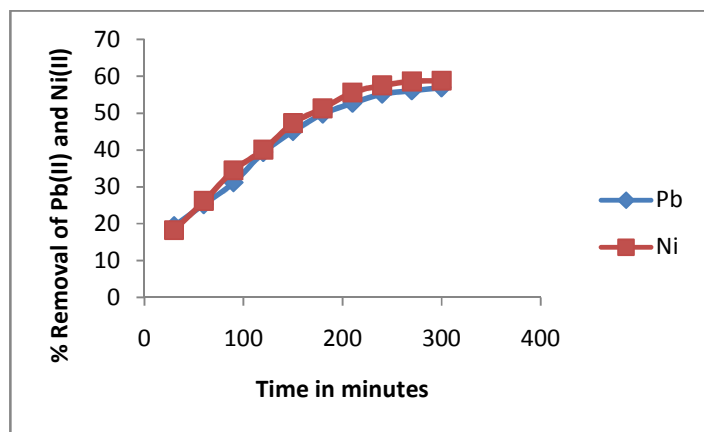


Fig 18 Effect of contact time on the removal of Pb(II) and Ni(II)

### Adsorption Isotherm Studies

#### Removal of Lead (II) and Nickel (II) ions by Chitosan-g-PAN copolymer

Table 2 Distribution of Pb(II) ion between sorbent and solution at equilibrium

Initial concentration of Pb(II) mg/L	1000	500	200	100	50
Initial amount of Pb(II) in 200ml soln.	200	100	40	20	10
Eqm adsorption in 1gm of sorbent (Ye)	43.8	31.2	20.3	10.8	6.5
Amt of Pb left in solution	156.2	68.8	19.7	9.2	3.5
Eqm con in 1000ml (Ce)	781	344	98.5	46	17.3
Ce/Ye	17.83	11.02	4.9	4.3	2.6

Table 3 Distribution of Ni(II) ion between sorbent and solution at equilibrium

Initial concentration of Ni(II) mg/L	1000	500	200	100	50
Initial amount of Ni(II) in 200ml soln.	200	100	40	20	10
Eqm adsorption in 1gm of sorbent (Ye)	30.4	19.4	10.3	9.7	5
Amt of Ni(II) left in solution	169.6	80.6	29.7	10.3	5
Eqm con in 1000ml (Ce)	848	403	148.5	51.5	25
Ce/Ye	27.8	21.3	14.4	5.3	5

#### Freundlich isotherm

The Freundlich isotherm equation is used for the description of multilayer adsorption with the interaction between adsorbed molecules. The model predicts that the adsorbate concentration in the solution will be increasing. The model applies to the adsorption onto heterogeneous surfaces with uniform energy distribution and reversible adsorption. The non-linear form of Freundlich equation may be written as

$$q_e = K_f C_e^{1/n_f}$$

The linearised form of Freundlich isotherm is given by the equation

$$\log q_e = \log K_f + 1/n_f \log C_e$$

where

$q_e$  = Amount adsorbed per unit weight of adsorbent at equilibrium ( $\text{mg g}^{-1}$ )

$C_e$  = Equilibrium concentration of adsorbate in solution after adsorption ( $\text{mg dm}^3$ )

$K_f$  = Empirical Freundlich constant or capacity factor ( $\text{mg g}^{-1}$ )

$1/n$  = Freundlich exponent

Non-linear behaviour of adsorption indicates that adsorption energy barrier increase exponentially with increasing fraction of filled sites on the adsorbent .

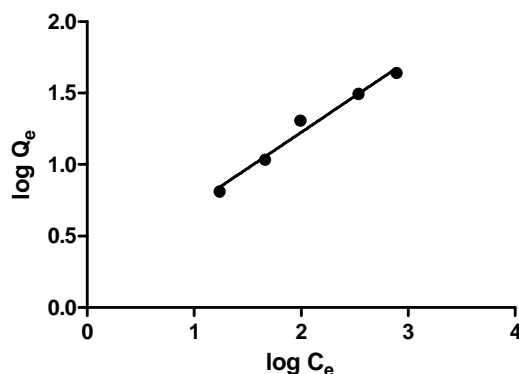


Figure 19 Effect of initial concentration on the Freundlich adsorption of Pb(II) ion by chitosan-g-PAN copolymer

log K	0.2197
1/n	0.5028

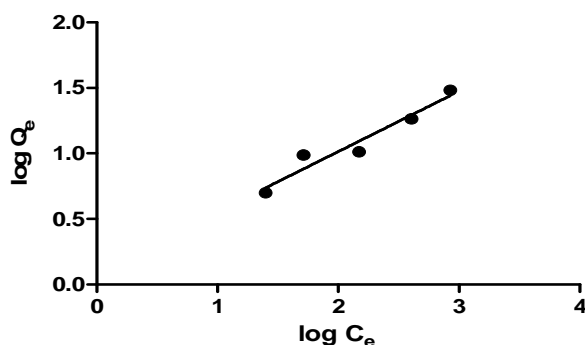


Figure 20 Effect of initial concentration on the Freundlich adsorption of Ni (II) ion by chitosan-g-PAN copolymer

log K	0.09331
1/n	0.4604

Table 4 The Freundlich isotherm parameters for Lead and Nickel on Chitosan-g-PAN copolymer

Metal ions	Freundlich Parameters		
	$K_f (\text{mg.g}^{-1})$	n	$R^2$
Pb(II)	1.6584	1.9888	0.9785
Ni(II)	1.2397	2.1720	0.9394

The Freundlich isotherm parameter  $1/n$  measures the adsorption intensity of metal ions on biosorbent. **Table 3.10** showed that the Freundlich constants  $K_f$  and  $n$  were 1.6584 and 1.9888 for lead and 1.2397 and 2.1720 for nickel. Other than homogeneous surface, the Freundlich equation is also suitable for a highly heterogeneous surface and an adsorption isotherm indicates the multilayer adsorption. The value of  $1/n$ , less than unity is an indication that significant adsorption takes place at low concentration but in the increase in the amount adsorbed with concentration becomes less significant at higher concentration and vice versa.

In the present study where CS-g-PAN was used as an adsorbent the n values between 1 -10 represent beneficial adsorption.

### 3.6.2 Langmuir Isotherm

The application of biosorption process on the commercial scale requires proper quantification of the sorption equilibrium for process simulation. The Langmuir equation has been frequently used to give the sorption equilibrium. The Langmuir isotherm represents the equilibrium distribution of metal ions between the solid and liquid phases. The Langmuir model assumes that the uptake of metal ions occurs on a homogenous surface by monolayer adsorption without any interaction between adsorbed ions. To get the equilibrium data, initial metal concentrations were varied while the adsorbent mass in each sample was kept constant. The linearised Langmuir isotherm allows the calculation of adsorption capacities and Langmuir constant by the following equation:

$$\frac{C_{eq}}{C_{ads}} = \frac{bC_{eq}}{K_L} + \frac{1}{K_L}$$

$$C_{max} = \frac{K_L}{b}$$

where

$C_{ads}$  = amount of metal ions adsorbed ( $\text{mg g}^{-1}$ )

$C_{eq}$  = equilibrium concentration of metal ion in solution ( $\text{mg dm}^{-3}$ )

$K_L$  = Langmuir constant ( $\text{dm}^3 \cdot \text{g}^{-1}$ )

$b$  = Langmuir constant ( $\text{dm}^3 \cdot \text{g}^{-1}$ )

$C_{max}$  = maximum metal ion to adsorb onto 1g adsorbent ( $\text{mg} \cdot \text{g}^{-1}$ )

The constant “b” in the Langmuir equation is related to the energy or the net enthalpy of the sorption process. The constant  $K_L$  can be used to determine the enthalpy of adsorption. The constants “b” and “ $K_L$ ” are the characteristics of the Langmuir equation and can be determined from the linearised form of the Langmuir equation. A linearised plot of  $C_{eq}/C_{ads}$  against  $C_{eq}$  gives “ $K_L$ ” and “b”.

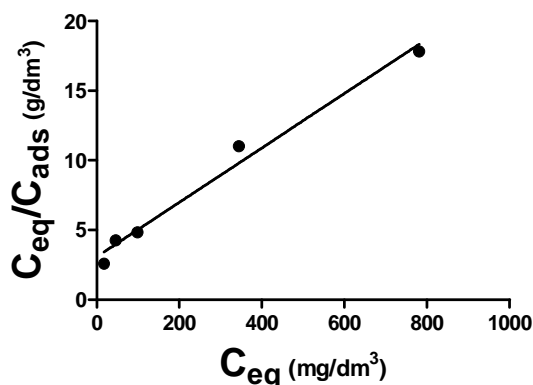


Figure 21 Effect of initial concentration on the Langmuir adsorption of Pb(II) by chitosan-g-PAN copolymer

Table 5 Adsorption isotherm constant,  $C_{max}$  and correlation coefficients

Metal ions	Langmuir constants			
	$K_L$ ( $\text{dm}^3 \cdot \text{g}^{-1}$ )	$b$ ( $\text{dm}^3 \cdot \text{mg}^{-1}$ )	$C_{max}$ ( $\text{mg g}^{-1}$ )	$R^2$
Pb(II)	3.080	0.01954	157.62	0.9842
Ni(II)	6.629	0.02770	239.314	0.9854

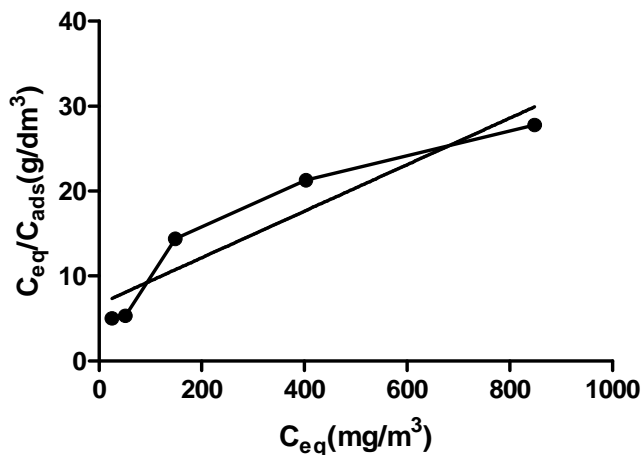


Figure 22 Effect of initial concentration on the Langmuir adsorption of Ni(II) by chitosan-g-PAN copolymer

Linear Langmuir plot indicates the formation of monolayer coverage of adsorbate on the surface of adsorbent.  $C_{max}$  value for nickel is high as compared to that of lead. The values are 239.314 mg of nickel per gram of chitosan-g-polyacrylonitrile and 157.62 mg of lead per gram of chitosan-g-polyacrylonitrile. Value of  $R^2$  shows correlation or linear relationship. The relationship becomes more linear with the values closer to 1. Thus, it is found that the adsorption of Pb(II) and Ni(II) onto chitosan-g-polyacrylonitrile correlates well with Langmuir equation.

The essential features of a Langmuir isotherm can be expressed in terms of a dimensionless constant separation factor or equilibrium parameter,  $R_L$  that is used to predict if an adsorption system is favourable or unfavourable.

The separation factor,  $R_L$  is defined by

$$R_L = \frac{1}{1 + bC_f}$$

where  $C_f$  is the final Pb(II) and Ni(II) concentration ( $\text{mg dm}^{-3}$ ) and  $b$  is the Langmuir adsorption equilibrium constant ( $\text{dm}^3 \text{mg}^{-1}$ ). The parameter indicates the isotherm shape according to **Table - 6**.

Table – 6 Effect of separation factor on isotherm shape

$R_L$ Values	Type of isotherm
$R_L > 1$	Unfavourable
$R_L = 1$	Linear
$0 < R_L < 1$	Favourable
$R_L = 0$	Irreversible

Table – 7  $R_L$  values based on Langmuir adsorption

Metal ions	Initial concentration $C_0$ ( $\text{mg/dm}^3$ )	Final concentration $C_f$ ( $\text{mg/dm}^3$ )	$R_L$ Values
Pb(II)	1000	781	0.0662
	500	344	0.1366
	200	98.5	0.3557
	100	46	0.5323
	50	17.3	0.7059
Ni(II)	1000	848	0.0408
	500	403	0.0822
	200	148.5	0.1955
	100	51.5	0.4121
	50	25	0.5908

The values of  $R_L$  calculated for different Pb(II) and Ni(II) concentration are given in **Table – 7**. As the values are in the range of  $0 < R < 1$ , it indicates that the adsorption of Pb(II) and Ni(II) onto chitosan-g-acrylonitrile is favourable. Thus, chitosan-g-polyacrylonitrile is an efficient adsorbent.

**Table – 8 Regression co-efficient ( $R^2$ ) comparison of two isotherms**

Metal ions	Regression co-efficient ( $R^2$ )	
	Langmuir isotherm	Freundlich isotherm
Lead	0.9842	0.9785
Nickel	0.9854	0.9394

The value of  $R^2$  can give more information about the suitability of adsorption model. The high values of the correlation coefficient ( $R^2 > 0.9$ ) showed that both the Langmuir and Freundlich isotherm equations can satisfactorily describe the adsorption of Pb(II) and Ni(II) onto chitosan-g-PAN copolymer.

Langmuir isotherms for Pb(II) and Ni(II) are shown in **Figures 21 and 22** and the related parameters of the isotherm are given in **Table 7**. Maximum adsorption capacity,  $C_{max}$  for complete monolayer coverage is 157.62 ( $\text{mg g}^{-1}$ ) for Lead and 239.314 ( $\text{mg g}^{-1}$ ) for Nickel.

Thus, the adsorption pattern of two metal ions on chitosan-g-PAN copolymer was well fitted by Langmuir as well as Freundlich isotherm in the experimental concentration range, according to the values of correlation coefficient,  $R^2$ . The Langmuir and Freundlich isotherm models provided the best fit for experimental data which indicated monolayer as well as multilayer adsorption.

## CONCLUSION

From the above results and discussion it became evident that the chitosan-g-PAN copolymer was prepared successfully. The FTIR, TGA, XRD, and SEM results confirm the formation of copolymer. The decrease in the crystallinity of the copolymers with reference to pure chitosan was proved by XRD studies. Both monolayer and multilayer adsorption of heavy metals lead and nickel was proved by conducting adsorption studies of chitosan-g-PAN copolymer by Langmuir and Freundlich adsorption isotherms. The prepared copolymer was used for the remediation of heavy metals in the wastewater. The copolymer was chosen for the batch adsorption studies by varying adsorbent dose, pH and contact time under optimized conditions and metal analyses were carried out and the results showed that the copolymer was an excellent adsorbent.

## REFERENCES

- [1] Sudha P N, Chitin, Chitosan, Oligosaccharides and Their Derivatives. Ed. SeKwon Kim CRC press, **2010**, 561576.
- [2] Malik A, *Environment International* ,**2004**, 30 261–278.
- [3] McCluggage D, Heavy Metal Poisoning, NCS Magazine, Published by The Bird Hospital, CO, U.S.A. ([www.cockatiels.org/articles/Diseases/metals.html](http://www.cockatiels.org/articles/Diseases/metals.html)), **2011**,44-56
- [4] Das K K, Gupta A D, Dhundasi S A, Patil A M, Das S N & Ambekar J G, *J Basic Clin Physiol Pharmacol*, **2006**, 17(1), 29-44.
- [5] Gray N F, Water Technology. John Wiley & Sons, New York, **1999**, 473–474.
- [6] Veglio F, Esposito A & Reverber A P, *Hydrometallurgy*, **2002**, 65, 43-57.
- [7] Tomko J, Backor M & Stofko M, *Acta Metallurgica Slovaca* , **2006**, 12 , 447-451.
- [8] Boddu V, Abburi K, Talbott J L & Smith E D *Environmental Science and Technology*, **2003**, 37 , 4449-4456.
- [9] Viera R H S F & Volesky B, *Internat. Microbiol.*,**2000** 3,17-24.
- [10] Volesky B & Schiewer S, Biosorption, Metals. Encyclopedia of Bioprocess Technology (Fermentation, Biocatalysis and Bioseparation), **2000**, 1, 433–453.
- [11] Acosta R I, Rodriguez X, Guitierrez C. & Motctezuma G, *Bioinorganic Chemistry and Applications*, **2004**, 2(1-2), 1-7.
- [12] Kubota Y & Kikuchi, Macromolecular complexes of chitosan in Polysaccharides, structural diversity and functional versatility. S. Dumitriu (Ed), Newyork, Deckker, **1999**, 595-628.
- [13] Sreenivasan K, *Journal of Applied Polymer Science*, **1998**, 69(6), 1051-1055.
- [14] Bailey S E, Olin T J, Bricka R M & Adrian D D, *Water Resource*, **1999**, 33(11), 2469-2479.

- [15] Gupta V K, Shrivastava A K & Jain N, *Water Resource*, **2001**, 35, 4079-4085.
- [16] Nayak P L & Lenka S, *Journal of Polymer Science—Polymer Chemistry Edition*, **1981**, 19, 1561.
- [17] Bolto B A, Soluble polymers in water purification. *Progress in Polymer Science*, **1995**, 20, 987-1041.
- [18] Khor E, *Material Science*, **2002**, 6, 313 – 317.
- [19] Hirano S, *Polymer International*, **1999**, 48, 732 – 734.
- [20] Crini G, *Progress in Polymer Science*, **2005**, 30, 38-70.
- [21] Alves N M & Mano J F, *International Journal of Biological Macromolecules*, **2008**, 43, 401-414.
- [22] Ramya R, Sankar P & Anbalagan S, *International Journal of Environmental Science*, **2011**, 6, 121-123.
- [23] Shanmugapriya A & Sudha P N, *International Journal of Environmental Science*, **2011**, 6, 133-135.
- [24] Jayakumar R, Prabakaran M, Reis R L & Mano J F, *Carbohydrate. Polym.* **2005**, 62, 142–158.
- [25] Rabindra K. Nanda, Subodh S. Patil and Dipak A. Navathar, *Der Pharma Chemica*, **2012**, 4(4), 1619-1625.